arXiv:0908.3887v1 [cond-mat.str-el] 26 Aug 2009

A Compact Treatment of the Friedel-Anderson and the Kondo Impurity Using the FAIR Method (**F**riedel **A**rtificially **I**nserted **R**esonance)

Gerd Bergmann
Department of Physics
University of Southern California
Los Angeles, California 90089-0484
e-mail: bergmann@usc.edu

August 26, 2009

Abstract

Although the Kondo effect and the Kondo ground state of a magnetic impurity have been investigated for more than forty years it was until recently difficult if not impossible to calculate spatial properties of the ground state. In particular the calculation of the spatial distribution of the so-called Kondo cloud or even its existence have been elusive. In recent years a new method has been introduced to investigate the properties of magnetic impurities, the FAIR method, where the abbreviation stands for Friedel Artificially Inserted Resonance. The FAIR solution of the Friedel-Anderson and the Kondo impurity problems consists of only eight or four Slater states. Because of its compactness the spatial electron density and polarization can be easily calculated. In this article a short review of the method is given. A comparison with results from the large N-approximation, the Numerical Renormalization Group theory and other methods shows excellent agreement. The FAIR solution yields (for the first time) the electronic polarization in the Kondo cloud.

1 Introduction

The properties of magnetic impurities in a metal is one of the most intensively studied problems in solid state physics. The work of Friedel [1] and Anderson [2] laid the foundation to understand why some transition-metal impurities form a local magnetic moment while others don't. Kondo [3] showed that multiple scattering of conduction electrons by a magnetic impurity yields a divergent contribution to the resistance in perturbation theory. Kondo's paper stimulated a large body of theoretical and experimental work which changed our understanding of d- and f-impurities completely (see for example [4], [5], [6], [7], [8], [9], [10], [11], [12], [13]). A large number of sophisticated methods were applied in the following three decades to better understand and solve the Kondo and Friedel-Anderson problems. In particular, it was shown that at zero temperature the Friedel-Anderson impurity is in a non-magnetic state. To name a few of these methods: scaling [14], renormalization [15], [16], [17], [18] Fermi-liquid theory [19], [20], slave-bosons (see for example [21]), large-spin limit [22], [23]. After decades of research exact solutions of the Kondo and Friedel-Anderson impurities were derived with help of the Bethe-ansatz [24], [25], [26], representing a magnificent theoretical achievement. The experimental and theoretical progress has been collected in a large number of review articles [7], [8], [9], [10], [11], [12], [13], [15], [20], [21], [23], [24], [25], [26], [27].

The exact theory of the Bethe ansatz is such a complex theory that only a limited number of parameters can be calculated. For the majority of practical problems one uses the numerical renormalization group (**NRG**) theory and the large-spin (large N) method. Recently the author introduced another approximate solution for the Friedel-Anderson (FA) [28], [29] and the Kondo impurity [30], the FAIR method. The FAIR solution consists of only four to eight Slater states and is therefore very compact. It is well suited to calculate in particular spatial properties of the Kondo ground state. It yields the first quantitative calculations of the Kondo cloud [31]. There are very few spatial properties of the Kondo ground state calculated with other theoretical approaches. One example is the NRG calculation for the Friedel oscillations in the vicinity of a Kondo impurity [32]. A calculation of the Friedel oscillations with the FAIR method yields good agreement with the NRG results [33]. In this short review the FAIR method will be introduced and some of the results presented. The FAIR method uses Wilson states [15] which replace a complete conduction electron band by a relatively small number of states which carry the full interaction with the impurity. The Wilson states are sketched in appendix A.

2 II The FAIR Method

2.1 The artificial Friedel resonance state

We consider the Hamiltonian of a band with a finite number N of non-interacting electron states

$$H_0 = \sum_{\nu=1}^{N} \varepsilon_\nu c_\nu^\dagger c_\nu$$

The $c_\nu^\dagger$ are the creation operators of the band. *In the following the states such as $c_\nu^\dagger\Phi_0$ are represented and addressed by their creation operators $c_\nu^\dagger$ suppressing the vacuum states Φ_0.* From these band states a new (arbitrary) state $a_0^\dagger$ is composed

$$a_0^\dagger = \sum_{\nu=1}^{N} \alpha_0^\nu c_\nu^\dagger \tag{1}$$

In the next step an intermediate basis $\left\{\overline{a}_i^\dagger\right\}$ can be constructed numerically where the additional $(N-1)$ states $\overline{a}_i^\dagger$ are orthonormal to each other and to $a_0^\dagger$. In this basis the Hamiltonian H_0 is given by an $N \times N$ matrix with the elements $(H_0)_{ij}$ where $(H_0)_{00}$ is at the left upper corner. In the final step the $(N-1) \times (N-1)$ sub-matrix of $(H_0)_{ij}$ for $i, j > 0$ is diagonalized. This yields the new basis $\left\{a_i^\dagger\right\} = \left\{a_0^\dagger, a_1^\dagger, a_2^\dagger, .., a_{N-1}^\dagger\right\}$ which is uniquely determined by the state $a_0^\dagger$. In this basis the s-band Hamiltonian has the form

$$H_0 = \sum_{\nu=1}^{N} E_i a_i^\dagger a_i + E_0 a_0^\dagger a_0 + \sum_{\nu=1}^{N} V_{fr}(i) \left(a_0^\dagger a_i + a_i^\dagger a_0\right) \tag{2}$$

One recognizes that this Hamiltonian is analogous to a Friedel Hamiltonian where $a_0^\dagger$ represents an artificial Friedel resonance. Therefore this state is called a FAIR state for **F**riedel **A**rtificially **I**nserted **R**esonance state.

It has to be emphasized that the FAIR state $a_0^\dagger$ can have any composition of the basis states $c_\nu^\dagger$. Therefore it can be adjusted to a given problem without any restriction. This gives the FAIR method its adaptability.

2.2 The Friedel resonance

As an example let us consider the simple Friedel resonance Hamiltonian H_{Fr}.

$$H_{FR} = \sum_{\nu=1}^{N} \varepsilon_\nu c_\nu^\dagger c_\nu + E_d d^\dagger d + \sum_{\nu=1}^{N} V_{sd}(\nu)[d^\dagger c_\nu + c_\nu^\dagger d] \tag{3}$$

Since H_{FR} does not depend on the spin the latter will be ignored. The first term is the conduction band Hamiltonian H_0, the second term gives the energy of the d (resonance) state of the impurity with $d^\dagger$ being its creation operator. The last term represents the interaction between the d state and the conduction electrons.

There exists a FAIR state $a_0^\dagger$ and a FAIR basis $\left\{a_i^\dagger\right\}$ so that the n-electron ground state of the Friedel Hamiltonian is exactly given by

$$\Psi_{Fr} = \left(A a_0^\dagger + B d^\dagger\right) \prod_{i=1}^{n-1} a_i^\dagger \Phi_0 \tag{4}$$

Here A and B are coefficients which fulfill the condition $A^2 + B^2 = 1$. Actually this exact form of the ground state of the Friedel impurity can be understood without any analytic or numerical calculation [34]. This is shown in the appendix D. In ref. [35] it was discovered by a variation of $a_0^\dagger$ minimizing the ground state energy of the state (4) with respect to the Friedel Hamiltonian (3). The state $a_0^\dagger$ determines all the other basis states $a_i^\dagger$ uniquely. Since the new basis $\left\{a_i^\dagger\right\}$ has the same number of states as the original basis $\left\{c_\nu^\dagger\right\}$ the construction of the basis $\left\{a_i^\dagger\right\}$ is only possible if the number N of basis states is small. For $N \approx 10^{23}$ it would be hard to construct the orthonormal sub-diagonal basis $\left\{a_i^\dagger\right\}$. Wilson has shown in his Kondo paper [15] how to construct a finite basis $\left\{c_\nu^\dagger\right\}$ which preserves the full interaction with the impurity. The Wilson states are discussed in the appendix A.

The example of the Friedel Hamiltonian shows the simplicity and effectiveness of the FAIR method. It can be applied to treat the Friedel-Anderson and the Kondo impurity.

3 The Friedel-Anderson impurity

The FA-Hamiltonian consists of the Friedel Hamiltonian (3) for both spins plus a Coulomb term of the form $H_{\mathrm{C}} = U n_{d\uparrow} n_{d\downarrow}$.

$$H_{FA} = \sum\nolimits_\sigma \left\{ \sum_{\nu=1}^{N} \varepsilon_\nu c_{\nu\sigma}^\dagger c_{\nu\sigma} + E_d d_\sigma^\dagger d_\sigma + \sum_{\nu=1}^{N} V_{sd}(\nu) [d_\sigma^\dagger c_{\nu\sigma} + c_{\nu\sigma}^\dagger d_\sigma] \right\} + U n_{d\uparrow} n_{d\downarrow} \tag{5}$$

3.1 The magnetic state

In the early years (before the Kondo paper) it was the goal to calculate (and measure) the magnetic moment of a d- or f-impurity. After the discovery of the Kondo effect and after Schrieffer and Wolff [36] transformed the FA-Hamiltonian into a Kondo Hamiltonian it became clear that the ground state of the FA impurity is non-magnetic. Then the calculation of the magnetic moment was often considered as irrelevant, even heresy. The paper by Krishna-murthy, Wilkins, and Wilson [17] clarified the role of the local magnetic moment in the FA-impurity. KWW performed a numerical renormalization a la Wilson [15] for the FA-Hamiltonian. They demonstrated that the renomalization-group flow diagram showed very different flows from the free-orbital fixed point $\mathrm{H}_{\mathrm{FO}}^*$ to the strong coupling fixed point $\mathrm{H}_{\mathrm{SC}}^*$ (see Fig.1). For sufficiently large Coulomb repulsion (when $U >> \Gamma = \pi\rho \left|V_{sd}\right|^2$) the flow of their Hamiltonian H_N passed close to the (unstable) fixed point $\mathrm{H}_{\mathrm{LM}}^*$ for a local moment. This means that under these conditions the impurity assumed first a magnetic moment when the temperature is lowered. After passing the fixed point for the local moment $\mathrm{H}_{\mathrm{LM}}^*$ the renormalization flow is essentially the same as for a Kondo Hamiltonian (where a local moment is the starting point).

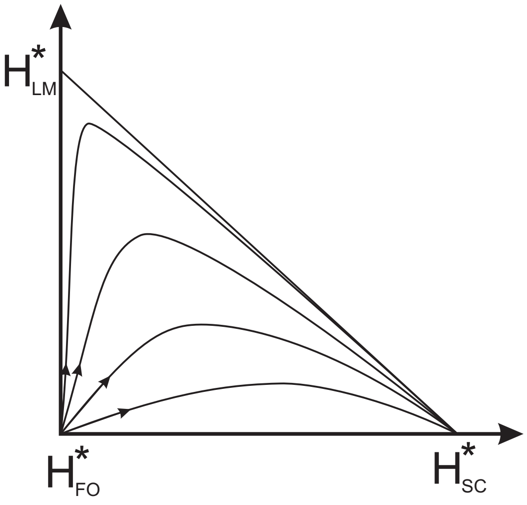

Fig.1:Schematic renormalization-group flow diagram after ref.[17].

With decreasing ratio of U/Γ the flow path passes less and less close to $\mathrm{H}^*_{\mathrm{LM}}$. This means that the size of the local moment decreases until there is no longer a local moment formed. (The flow of the susceptibility indicates this behavior).

At the end point of the renormalization the system approaches the strong coupling fixed point $\mathrm{H}^*_{\mathrm{SC}}$ and shows the universal behavior of the Kondo ground state. Nevertheless the ground-state wave functions are quite different for small and large ratios of U/Γ because the size of the magnetic moment is engraved into the wave function.

Let us first consider the local moment state of the FA-impurity. This state is a ground state if one applies a magnetic field which is strong enough to suppress the Kondo ground state. Within the FAIR approach the (potentially) magnetic solution has the form

$$\Psi_{MS}=\left[A_{a,b}a_{0\uparrow}^{\dagger}b_{0\downarrow}^{\dagger}+A_{a,d}a_{0\uparrow}^{\dagger}d_{\downarrow}^{\dagger}+A_{d,b}d_{\uparrow}^{\dagger}b_{0\downarrow}^{\dagger}+A_{d,d}d_{\uparrow}^{\dagger}d_{\downarrow}^{\dagger}\right]\prod_{i=1}^{n-1}a_{i\uparrow}^{\dagger}\prod_{i=1}^{n-1}b_{i\downarrow}^{\dagger}\Phi_{0} \tag{6}$$

where $\left\{a_i^\dagger\right\}$ and $\left\{b_i^\dagger\right\}$ are two (different) FAIR bases of the N-dimensional Hilbert space. The state (6) opens a wide playing field for optimizing the solution: (i) The FAIR states $a_{0\uparrow}^\dagger$ and $b_{0\downarrow}^\dagger$ can be individually optimized, each one defining a whole basis $\left\{a_i^\dagger\right\}$, $\left\{b_i^\dagger\right\}$ and (ii) the coefficients $A_{a,b}, A_{a,d}, A_{d,b}, A_{d,d}$ can be optimized fulfilling only the normalization condition $A_{a,b}^2+A_{a,d}^2+A_{d,b}^2+A_{d,d}^2=1$. Since the relative size of the coefficients $A_{a,b}$, $A_{a,d}$, $A_{d,b}$ and $A_{d,d}$ is not restricted this solution describes correlation effects well. The optimization procedure is described in detail in the appendix B.

Fig.2 shows the structure of the four Slater states of Ψ_{MS} graphically. The FAIR states $a_0^\dagger$ and $b_0^\dagger$ are imbedded in the spin-up and down bands while the $d_\uparrow^\dagger$ and $d_\downarrow^\dagger$ states are shown on the left and right side of the bands. Full circles represent occupied states.

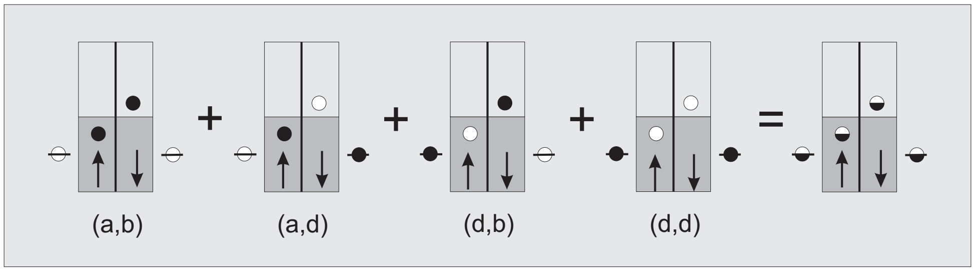

Fig.2: The composition of the magnetic state Ψ_{MS} is shown. It consists of four Slater states. Each Slater state has a half-filled spin-up and down band, two FAIR states (circles in within the bands) and two d-states (circles on the left and right of the band). Full black circles represent occupied states and white circles represent empty states. The band at the right with the half-filled circles symbolizes the magnetic solution with four Slater states.

Fig.3a shows the magnetic moment as a function of U for the mean-field solution and the magnetic state Ψ_{MS}. In Fig.3b the ground-state energies of the mean-field solution and the magnetic state are compared. The magnetic FAIR solution has a considerably lower energy expectation value than the mean-field solution. More importantly it increases the critical value of U for the formation of a magnetic moment by almost a factor two (compared with the mean-field solution). The mean-field approximation is still used in combination with spin-density functional theory (SDFT) to calculate the magnetic moment of impurities [37], [38], [39], [40], [41]. A combination between SDFT and the FAIR solution appears to be very desirable.

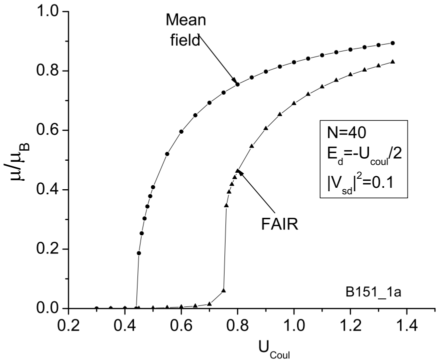

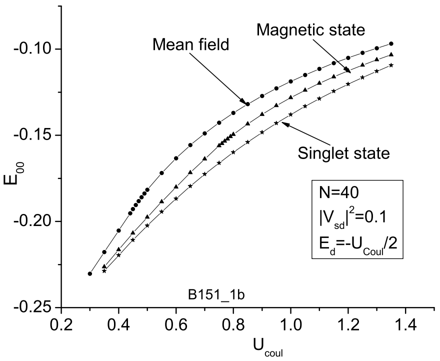

Fig.3a: The magnetic moment as a function of the Coulomb exchange energy U, using the mean-field solution and the magnetic FAIR solution Ψ_{MS}.

Fig.3b: The ground-state energies of the mean-field solution, the magnetic and the singlet FAIR solution

3.2 The singlet state

In hindsight it is quite natural that the magnetic state with its broken symmetry is not the ground state. By reversing all spins one obtains a new state with the same energy. In Fig.4 the energy of the magnetic state is plotted as a function of the magnetic moment.

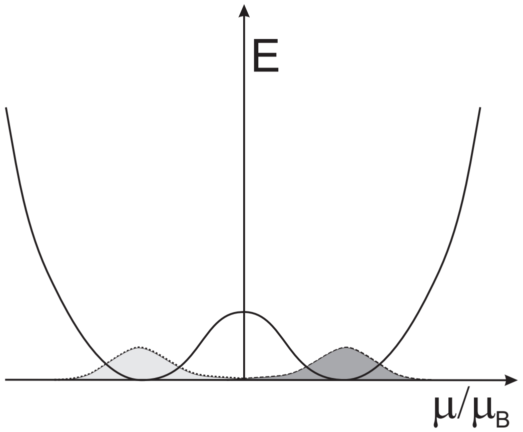

Fig.4: The energy of the FA impurity as a function of the magnetic moment.

This is a situation similar to an atom in a double well potential. In the ground state the atom is in a symmetric superposition of the wave functions in the two wells. In analogy one can construct the singlet ground state Ψ_{SS} of the FA-Hamiltonian. This state is obtained by reversing all spins in (6) and combining the two wave functions

$$\Psi_{SS} = \overline{\Psi_{MS}\left(\uparrow\right)} + \overline{\overline{\Psi_{MS}\left(\downarrow\right)}}$$

$$= \left[\overline{A_{a,b}} a_{0\uparrow}^{\dagger} b_{0\downarrow}^{\dagger} + \overline{A_{a,d}} a_{0\uparrow}^{\dagger} d_{\downarrow}^{\dagger} + A_{d,b} d_{\uparrow}^{\dagger} b_{0\downarrow}^{\dagger} + A_{d,d} d_{\uparrow}^{\dagger} d_{\downarrow}^{\dagger}\right] \prod_{i=1}^{n-1} a_{i\uparrow}^{\dagger} \prod_{i=1}^{n-1} b_{i\downarrow}^{\dagger} \Phi_0 \tag{7}$$

$$+ \left[\overline{\overline{A_{a,b}}} b_{0\uparrow}^{\dagger} a_{0\downarrow}^{\dagger} + \overline{\overline{A_{a,d}}} d_{\uparrow}^{\dagger} a_{0\downarrow}^{\dagger} + \overline{\overline{A_{d,b}}} b_{0\uparrow}^{\dagger} d_{\downarrow}^{\dagger} + \overline{\overline{A_{d,d}}} d_{\downarrow}^{\dagger} d_{\uparrow}^{\dagger}\right] \prod_{i=1}^{n-1} b_{i\uparrow}^{\dagger} \prod_{i=1}^{n-1} a_{i\downarrow}^{\dagger} \Phi_0$$

Again one has to optimize $a_0^{\dagger}$, $b_0^{\dagger}$ and all the coefficients. It is remarkable that the composition of the FAIR states changes dramatically for small energies. The ground-state energy of the singlet FAIR solution lies considerably below that of the magnetic FAIR solution Ψ_{MS} (see Fig.3b). One can compare this ground-state energy with a set of numerical calculations by Gunnarsson and Schoenhammer [42]. They applied the large N_f method to the (non-degenerate) FA-Hamiltonian (spin 1/2) for a finite Coulomb interaction and included double occupancy of the impurity level. They calculated the ground-state energy in the $1/N_f$-expansion up to the order $(1/N_f)^2$ which includes more than 10^7 basis states. For the s-d-hopping transition they used an elliptic form. With the following parameters:

band width $B_{GS} = 6eV$, Coulomb energy $U_{GS} = 5eV$, d-state energy $E_{d,GS} = -2.5eV$ they performed two calculations, one for s-d coupling $V_{GS} = 1eV$ and another for $V_{GS} = 2eV$. The table compares the ground-state energies and the occupation for of the d-states (d_0, d_1, d_2) obtained by GS and the FAIR for $V_{GS} = 1eV$ and $2eV$. Not only the ground-state energies but also the occupation of the d-states agree remarkably well.

	states	E_0 [eV]	d_0	d_1	d_2	no. of coeff.
$V_{GS} = 1eV$	GS	-0.245	0.034	0.931	0.034	>10^7
	FAIR	-0.239	0.035	0.931	0.034	80

	states	E_0 $[eV]$	d_0	d_1	d_2	no. of coeff.
$V_{GS} = 2eV$	GS	-1.217	0.137	0.732	0.132	$> 10^7$
	FAIR	-1.234	0.140	0.722	0.138	80

Table Ia,b: The ground-state energy E_0 and the occupations d_0, d_1, d_2 of the d-states with 0,1 or 2 electrons.

It is worthwhile to remember that the FAIR solution is completely determined by the two FAIR states $a_0^\dagger$ and $b_0^\dagger$, i.e. by 2×40 amplitudes for a typical value of $N = 40$. On the other hand the large N calculation describes the ground state by more than 10^7 parameter, i.e., amplitudes of Slater states.

4 The Kondo Impurity

The Kondo Hamiltonian is a limiting case of the FA-Hamiltonian [36]. It applies when the exchange energy U approaches infinity while the d-state energy approaches $-\infty$, for example $E_d = -U/2$. Then the d-state is always singly occupied, either with spin up or down. The interaction between the spin $\mathbf{s}$ of a conduction electron and the spin $\mathbf{S}$ of the impurity can be expressed in the form $2J\mathbf{s} \cdot \mathbf{S}$ where $J > 0$.

In this case the ansatz for the compact FAIR-solution can be obtained from equ. (7). The coefficients $\overline{A_{a,b}}, \overline{\overline{A_{a,b}}}$; $A_{d,d}, \overline{\overline{A_{d,d}}}$ have to vanish because there is only single occupancy of the d-state in the Kondo solution. This yields

$$\Psi_K = \left[\overline{A_{a,d}} a_{0\uparrow}^\dagger d_\downarrow^\dagger + \overline{A_{d,b}} d_\uparrow^\dagger b_{0\downarrow}^\dagger\right] \prod_{i=1}^{n-1} a_{i\uparrow}^\dagger \prod_{i=1}^{n-1} b_{i\downarrow}^\dagger \Phi_0 \qquad (8)$$

$$+ \left[\overline{\overline{A_{a,d}}} d_\uparrow^\dagger a_{0\downarrow}^\dagger + \overline{\overline{A_{d,b}}} b_{0\uparrow}^\dagger d_\downarrow^\dagger\right] \prod_{i=1}^{n-1} b_{i\uparrow}^\dagger \prod_{i=1}^{n-1} a_{i\downarrow}^\dagger \Phi_0$$

Again one can optimize the localized states $a_0^\dagger$ and $b_0^\dagger$ and the coefficients $\overline{A_{a,d}}, \overline{\overline{A_{a,d}}}, \overline{A_{d,b}}, \overline{\overline{A_{d,b}}}$. If one arranges the spin up to the left and spin down to the right in all components of (7) then one obtains in the ground state $\overline{A_{a,d}} = \overline{\overline{A_{a,d}}}$ and $\overline{A_{d,b}} = \overline{\overline{A_{d,b}}}$. Our group calculated the total spin of this state (for $J = 0.1$) and obtained for the expectation value of $\langle \mathbf{S}^2 \rangle = \left\langle (\mathbf{s}_d + \sum_i \mathbf{s}_i)^2 \right\rangle$ the value 0.04 in the ground state [30]. For the first excited state one obtains $\langle \mathbf{S}^2 \rangle = 1.99$. This means that the ground state is essentially a singlet state ($\langle \mathbf{S}^2 \rangle = 0$) and the first excited state a triplet state ($\langle \mathbf{S}^2 \rangle = 2$).

In the Kondo effect one is generally not so much interested in the ground-state energy but in the so-called Kondo energy. This is, for example, the energy difference between the triplet and singlet states. The logarithm of this excitation energy is plotted in Fig.5 as a function of $1/(2J\rho_0)$ as the full circles (ρ_0 is the density of states). The straight line corresponds to $\Delta E \approx 5D \exp\left[-1/(2J\rho_0)\right]$. This is the unrelaxed singlet-triplet energy which uses for the triplet state the same bases $\left\{ a_i^\dagger \right\}$ and $\left\{ b_i^\dagger \right\}$ as in the singlet state. One can derive a relaxed triplet state by the following trick. In the triplet state the coefficients are related by $\overline{\overline{A_{a,d}}} = -\overline{A_{a,d}}$ and $\overline{\overline{A_{d,b}}} = -\overline{A_{d,b}}$. If one replaces $\overline{\overline{A_{a,d}}}$, $\overline{\overline{A_{d,b}}}$ from the start by $-\overline{A_{a,d}}$, $-\overline{A_{d,b}}$ and optimizes the energy then one obtains the relaxed triplet energy. The difference between this energy and the singlet energy yields the relaxed excitation energy ΔE_{st}. (Since these are two independent calculations they have to be performed with an absolute accuracy of 10^{-10}). This relaxed excitation energy is plotted in Fig.5 as stars. The stars lie between two theoretical curves: (i) $\Delta E_{st} = D \exp\left[-1/(2J\rho_0)\right]$, given by the dashed curve and (ii) $\Delta E_{st} = \sqrt{2J\rho_0} D \exp\left[-1/(2J\rho_0)\right]$, given by the dotted curve. Both expressions are given in the literature as approximate values for the Kondo temperature $k_B T_K$. The numerical values lie closer to the second expression. Therefore the relaxed singlet-triplet excitation energy corresponds closely to the Kondo energy and confirms that the FAIR method represents the physics of the Kondo impurity accurately.

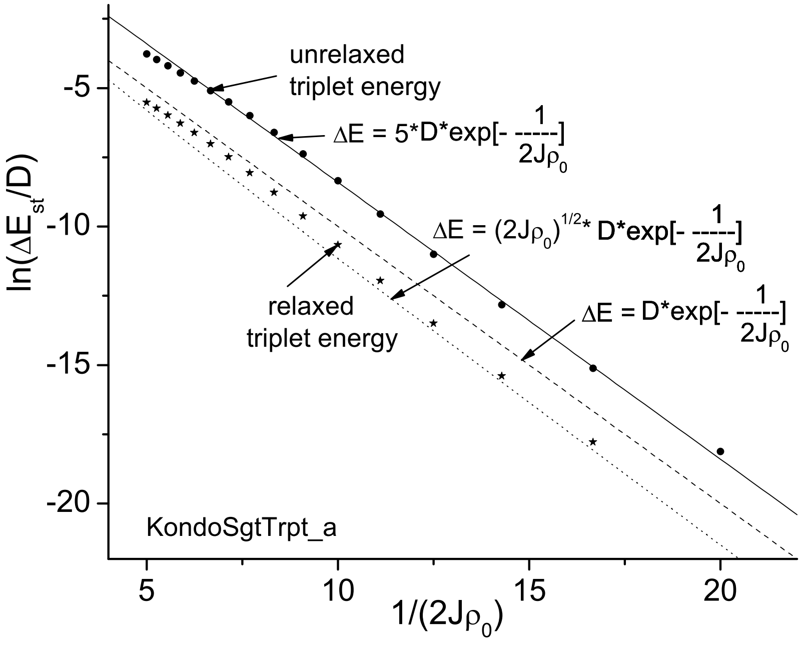

Fig.5: The energy difference between the singlet and triplet states. The full circles represent the unrelaxed singlet-triplet excitation energy ΔE_{st} while the stars yield the relaxed singlet-triplet excitation energy ΔE_{st}^{*} (see text). The dashed and dotted curves are theoretical expressions for the Kondo energy.

The FAIR method yields **both** energies, the ground-state and the singlet-triplet excitation energy, with good accuracy although the two energies can differ by a factor of thousand.

5 Real Space Properties

Since the compositions of the magnetic state and the singlet state are explicitly known and consist only of a few Slater states it is straight forward to calculated the electron density and spin polarization of the different states. The details of the calculation are described in ref. [31].

In Wilson's approach the wave number k is given in units of the Fermi wave number k_F. Therefore it is convenient to measure real space distances ξ in units of $\lambda_F/2$, i.e, half the Fermi wave length. (In this unit the wave length of the Friedel and RKKY oscillations is "1").

The density of the Wilson states $\psi_\nu(\xi)$ is given by

$$\rho_\nu^0(\xi) = |\psi_\nu(\xi)|^2 = 2^{\nu+3}\frac{\sin^2\left(\pi\xi\frac{1}{2^{\nu+2}}\right)}{\pi\xi}d\xi$$

(for $\nu < N/2$). The main contribution to the density ρ_ν^0 of the state ψ_ν lies roughly in the region $|\xi| < 2^{\nu+2}$ (in units of $\lambda_F/2$). The different $\psi_\nu(\xi)$ have very different electron densities and vary by roughly a factor of $2^{N/2}$ (which is generally larger than 10^6). Therefore it is useful to calculate the integrated electron density on a logarithmic scale.

First we discuss the magnetic state whose wave function is given in equ.(6).

5.1 The Magnetic State

The magnetic state Ψ_{MS} is the building block of the singlet state. Its multi-electron state is built from four Slater states and shown in equ. (6). The electron system has already a finite density without the d-impurity. Therefore it is useful to calculate the change of the (integrated) densities for spin-up and down conduction electrons due to the d-impurity.

In Fig.5 these (integrated) densities as well as their sum and difference (total density and polarization) are plotted for the parameters $E_d = -0.5$, $|V_{sd}^0|^2 = 0.04$, $U = 1$ and $N = 50$. With these parameters the impurity has a well developed magnetic moment of $\mu = 0.93\mu_B$. The occupation of the different components is $A_{a,b}^2 = 0.0294$, $A_{a,d}^2 = 0.0057$, $A_{d,b}^2 = 0.9355$ and $A_{d,d}^2 = 0.0294$. This means that 93.6% of the densities is due to the Slater state $\Psi_{d,b} = d_\uparrow^\dagger b_{0\downarrow}^\dagger \prod_{i=1}^{n-1} a_{i\uparrow}^\dagger \prod_{i=1}^{n-1} b_{i\downarrow}^\dagger \Phi_0$. The abscissa is the logarithm (using the basis 2) of $\xi = 2x/\lambda_F$.

The region beyond $\xi = 2^{20}$ corresponds to the rim or surface of the sample and is discussed below. One recognizes that there is only a negligible polarization of the electron gas in the vicinity of the impurity. The important result of Fig.5 is that there is no polarization cloud around the magnetic state of the impurity.

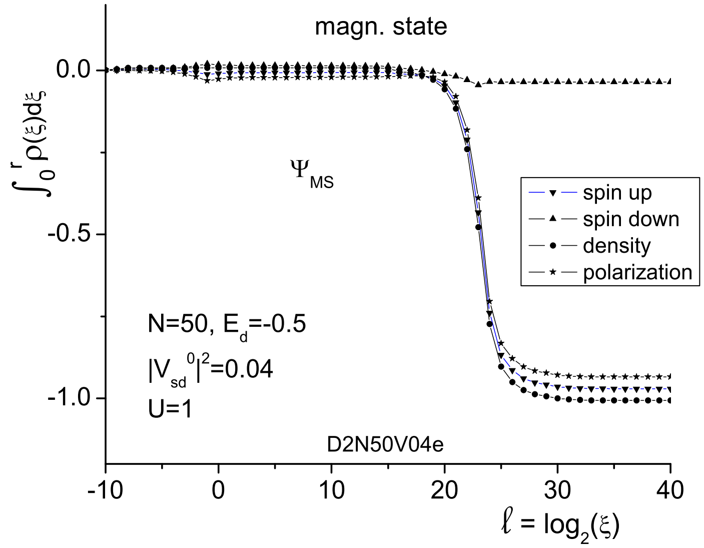

Fig.5: The net integrated density $\int_0^r \rho(\xi)\, d\xi$ of the s-electron within a distance r from the impurity for spin up and down, as well as total density and spin polarization. The magnetic moment of the impurity is $0.93\mu_B$.

If one looks at the magnetic state, in particular the dominant component $\Psi_{d,b} = d_\uparrow^\dagger b_{0\downarrow}^\dagger \prod_{i=1}^{n-1} a_{i\uparrow}^\dagger \prod_{i=1}^{n-1} b_{i\downarrow}^\dagger \Phi$ then one realizes that the total magnetic moment of all the conduction electrons is equal to $-1\mu_B$ (cancelling the moment of $+1\mu_B$ of the d-electron which is not shown in Fig.5). So how can the state Ψ_{MS} have a finite magnetic moment. The answer is given by Fig.5. The moment μ_B of the s-electrons is pushed towards the surface of the sample which is at the largest radius used for the Wilson states, i.e. $2^{N/2}$. This explains the change of the integrated densities and polarization at $l \approx 22$ from zero to -1. If one increases the number N of Wilson states by ΔN then the transition is shifted by $\Delta l = \Delta N/2$.

5.2 The Kondo cloud

One of the most controversial aspects of the Kondo ground state is the so-called Kondo cloud within the radius r_K where r_K is called the Kondo length

$$r_K = \frac{\hbar v_F}{\varepsilon_K} = \frac{d\varepsilon/dk}{\varepsilon_K} \tag{9}$$

(ε_K= Kondo energy, v_F = Fermi velocity of the s-electrons). For a linear dispersion relation this yields in reduced units $\xi_K = 1/\left(\pi\varepsilon_K\right)$ where in this relation the Kondo energy is given in units of the half-band width.

The idea is to divide the ground state Ψ_K of a Kondo impurity into two parts with opposite d-spins. The proponents of the Kondo cloud argue that in each component there is an s-electon cloud within the Kondo sphere which compensates the d-spin. An important assumption of the Kondo-cloud proponents is that, above the Kondo temperature, the bond is broken and this screening cloud evaporates from the Kondo sphere.

In the 1970's Slichter and co-workers [43] investigated Cu samples with dilute Fe-Kondo impurities by means of nuclear magnetic resonance. They did not detect any Kondo cloud. In a number of recent theoretical papers [44], [45], [46], [47] the argument is made that the old NMR experiments could not possibly have detected the screening electron because of the large volume of the Kondo sphere yielding a polarization of less than 10^{-8} electron spins per host atom.

The FAIR solution of the singlet ground state is well suited to determine the electron density and polarization in real space [31]. To the knowledge of the author this is the first detailed calculation of the Kondo cloud.

In the following analysis of the singlet state Ψ_{SS} the same parameters are used as for the magnetic state in Fig.5: $E_d = -0.5$, $|V_{sd}^0|^2 = 0.04$, $U = 1$. This yields the following squared amplitudes: $\overline{A_{a,b}^2} = 0.0146$, $\overline{A_{a,d}^2} = 0.0028$, $\overline{A_{db}^2} = 0.4629$ and $\overline{A_{dd}^2} = 0.0146$. (The $\overline{\overline{A_{x,y}}}$ amplitudes are identical). These occupations are very close to half the values of the magnetic state ($A_{s,s}^2 = 0.0294$, $A_{s,d}^2 = 0.0057$, $A_{d,s}^2 = 0.9355$ and $A_{d,d}^2 = 0.0294$). This means that Ψ_{SS} is given in good approximation as $\Psi_{SS} \approx \left(1/\sqrt{2}\right)\left[\overline{\Psi_{MS}(\uparrow)} + \overline{\overline{\Psi_{MS}(\downarrow)}}\right]$. The two magnetic states with d-spin up and down are robust building blocks of the singlet state. (However, there are subtle changes in the FAIR states which will be discussed below). Therefore the spin polarization of one of the magnetic components, for example of $\overline{\Psi_{MS}(\uparrow)}$, would be of interest.

In Fig.6 the integrated densities of spin up and down electrons, their sum and difference (the polarization) are plotted versus the distance from the magnetic impurity (on a logarithmic scale). One recognizes that now one has considerable contributions to the integrated net densities of both spins. The polarization of the two contributions is no longer zero but reaches a value of -0.46 at a distance of $r \approx 2^{11.6}$. Since the magnetic state $\overline{\Psi_{MS}(\uparrow)}$ with net d-spin up has only a weight of about 1/2 it contributes an effective $d_\uparrow^\dagger$-moment of $0.93/2 \approx 0.46$. Therefore this d-spin is well compensated by the polarization of the s-electron background.

The difference with the pure magnetic state is particularly striking. We observe a screening polarization cloud of s-electrons about the impurity within the range of $\xi \approx 2^{11.6}$ or $r =$

$3.1\times10^{3}\left(\lambda_F/2\right)$ .This is about the Kondo length r_K.

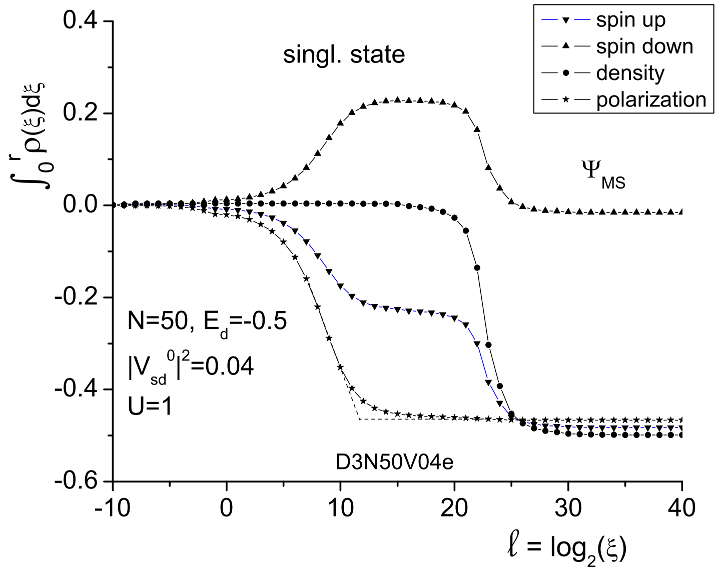

Fig.6: The net integrated density $\int_0^r \rho(x)\,dx$ within a distance $\xi = 2^l$ from the d-spin up component of the impurity. Shown are the spin up, spin down components as well as the total density and the polarization. The $d_\uparrow$-spin of 0.93/2 is screened by 0.46 s-electrons within the range of $\xi \approx 2^{11.6}$ (or $r \approx 3\times10^{3}\lambda_F/2$).

The polarization cloud for the ground state of the Kondo impurity (8) is in principle identical with the results for the Friedel-Anderson impurity and is discussed in detail in ref. [31].

5.3 Friedel Oscillation

Recently Affleck, Borda and Saleur (ABS) [32] showed that the Friedel oscillations due to a Kondo impurity are essentially suppressed within a distance of the order of the Kondo length r_K. They supported their theory by numerical calculations using NRG. Fig.7a shows the universal behavior of their numerical results for many different interaction strengths. Plotted is a function $F\left(\xi/\xi_K\right)$ (The actual amplitude is proportional to $[1-F]\,\xi^{-D}$ where D is the dimension of the system). For $F=1$ the Friedel oscillation is canceled while for $F=-1$ its amplitude is doubled). The author could not resist the temptation to evaluate the Friedel oscillations with the FAIR method [33]. Fig.7b shows the FAIR results of the amplitude $(1-F)$ of the Friedel oscillation for two different interaction strengths. This universal curve is shown in Fig.7a as the full blue curve. It agrees well with the numerical results by ABS. (The exact form of $F\left(\xi/\xi_K\right)$ is not known explicitly).

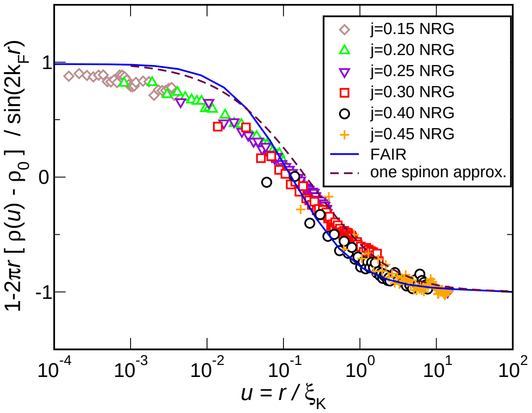

Fig.7a: Reduction $F\left(\xi/\xi_K\right)$ of the Friedel oscillation is plotted versus ξ/ξ_K. The amplitude is proportional to $\left[1-F\left(\xi/\xi_K\right)\right]$. Calculated by ABS.

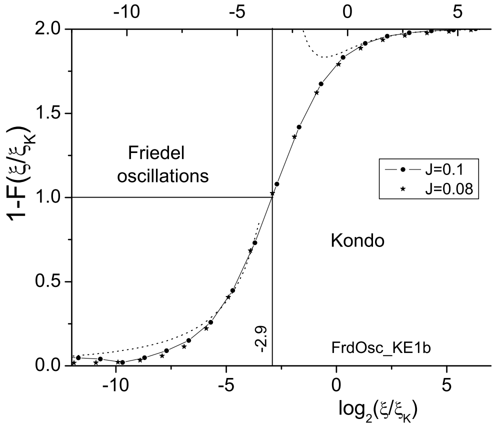

Fig.7b: The amplitude $\left[1-F\left(\xi/\xi_K\right)\right]$ of the Friedel oscillation for two different Kondo energies (from FAIR).

6 The FAIR States

At the heart of the FAIR approach are the FAIR states $a_0^\dagger$ and $b_0^\dagger$. Therefore a detailed discussion of these states is appropriate. The FAIR states are expressed in terms of the Wilson states. The latter are described in appendix A and a basic knowledge is required to follow some of the arguments of this paragraph.

A FAIR state is given as $a_0^\dagger=\sum_\nu \alpha_0^\nu c_\nu^\dagger$ where the states $c_\nu^\dagger$ are Wilson states. Now each Wilson state $c_\nu^\dagger$ represents all the original band states $\varphi_k^\dagger$ within the energy cell $\mathfrak{C}_\nu$ with an energy width Δ_ν where $\Delta_\nu=\left(\zeta_{\nu+1}-\zeta_\nu\right)$. The composition of the Wilson states $c_\nu^\dagger$ is $c_\nu^\dagger{=}Z_\nu{}^{-1/2}\sum_k \varphi_k^\dagger$. This yields for the FAIR state the composition

$$a_0^\dagger=\sum_\nu \sum_k \frac{\alpha_0^\nu}{\sqrt{Z_\nu}}\varphi_k^\dagger$$

This means that the FAIR state $a_0^\dagger$ consists of the original s-band states $\varphi_k^\dagger$ which have the amplitude of $\alpha_0^\nu/\sqrt{Z_\nu}$ in the energy cell $\mathfrak{C}_\nu$ or the occupation $\left|\alpha_0^\nu\right|^2/Z_\nu$. Now we can express

$$\frac{\left|\alpha_0^\nu\right|^2}{Z_\nu}=\frac{1}{Z}\frac{Z}{Z_\nu}\left|\alpha_0^\nu\right|^2=\frac{2}{Z}\frac{\left|\alpha_0^\nu\right|^2}{\Delta_\nu}$$

where Z is the total number of $\varphi_k^\dagger$ states in the conduction electron band (for one spin) and $Z/Z_\nu=2/\Delta_\nu$

Therefore the expression $p_\nu = |\alpha_0^\nu|^2 / \Delta_\nu$ represents (besides the factor $Z/2$) the composition of the FAIR state $a_0^\dagger$ in terms of the original band state $\varphi_k^\dagger$ in the energy cell $\mathfrak{C}_\nu$.

If one plots p_ν as a function of energy then one finds a step function because of the finite energy width of the cells $\mathfrak{C}_\nu$ of the Wilson states. If one repeatedly sub-divides the energy cells (doubling the number of Wilson states) then a smooth function $p(\zeta)$ emerges. This yields the FAIR state $a_0^\dagger$ ($b_0^\dagger$) in a quasi-continuous energy band. A rather good approximation of $p(\zeta)$ can be obtained by interpolation.

A comparison of Fig.5 and Fig.6 for the polarization of the magnetic state $\Psi_{MS}(\uparrow)$ and the magnetic component $\overline{\Psi_{MS}(\uparrow)}$ of the singlet state Ψ_{SS} shows a remarkable difference in the polarization about the impurity although the structure of the two states is identical. This is particularly surprising since the coefficients $\overline{A_{\alpha,\beta}} = \overline{\overline{A_{\alpha,\beta}}}$ in the singlet state are roughly $1/\sqrt{2}$ of the coefficients $A_{\alpha,\beta}$ of the magnetic state. However, in the singlet state one has a finite coupling between $\overline{\Psi_{MS}(\uparrow)}$ and $\overline{\overline{\Psi_{MS}(\downarrow)}}$. This shifts the composition of the FAIR states $a_0^\dagger$ and $b_0^\dagger$ towards small energies. The difference is that the FAIR states in the two states have a very different composition. To demonstrate this difference in the compositions $p_\nu = |\alpha_0^\nu|^2 / \Delta_\nu$ of $a_0^\dagger$ (and $b_0^\dagger$) are plotted in Fig.8 as a function of ν for the two different states.

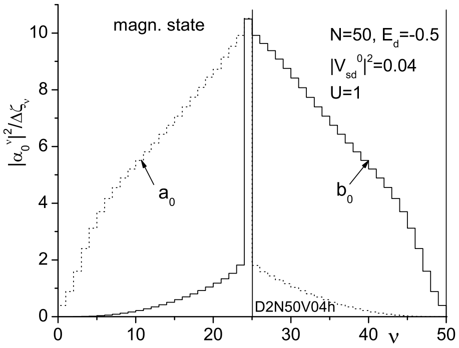

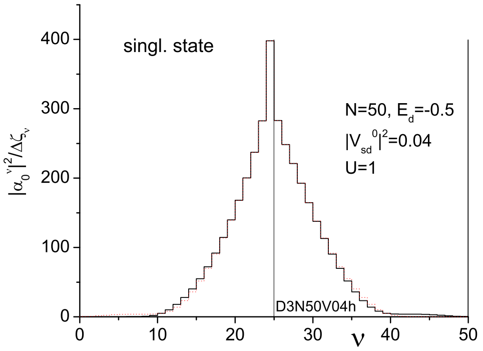

Fig.8a: The density distribution of the $p_\nu = \left|\alpha_{0\pm}^\nu\right|^2 / \Delta_\nu$ for the magnetic state Ψ_{MS} as a function of as a function of ν.

Fig.8b: The density distribution of the $p_\nu = \left|\alpha_{0\pm}^\nu\right|^2 / \Delta_\nu$ for the singlet ground state Ψ_{SS} as a function of the cell number ν. Note the difference in scale.

It would be more natural to plot p_ν as a function of the energy $p(\zeta)$. But for ν close to $N/2$ the width of the energy cells $\mathfrak{C}_\nu$ is less than 10^{-6} and any dependence of $p(\zeta)$ on the energy cannot be resolved on a linear scale. The probability p_ν increases close to the Fermi energy.

In Fig.8a for the magnetic state the compositions of $a_0^\dagger$ and $b_0^\dagger$ resemble mirror images. The function p_ν has a maximum at small energies of about 10.

In Fig.8b the corresponding plot is shown for the singlet state. The weight $p_\nu = |\alpha_0^\nu|^2 / \Delta_\nu$ close to the Fermi level is very different for the singlet state and the magnetic state. One observes in the singlet state a maximum of about 400 and the weights p_ν in $a_0^\dagger$ and $b_0^\dagger$ are essentially identical and not mirror images. The magnetic component of the singlet state is in a subtle way different from the magnetic state.

It should be emphasized again that the two states $a_0^\dagger$ and $b_0^\dagger$ contain the whole information about the many electron states Ψ_{MS} or Ψ_{SS}. When $a_0^\dagger$ and $b_0^\dagger$ are known the whole bases $\left\{a_i^\dagger\right\}$and $\left\{b_i^\dagger\right\}$ and all the coefficients $A_{\alpha,\beta}$ or $\overline{A_{\alpha,\beta}}, \overline{\overline{A_{\alpha,\beta}}}$ can be reconstructed.

One important advantage of the FAIR method is that one can modify the size of the energy cells $\mathfrak{C}_\nu$ after one has completed the numerical calculation of the FAIR states and the ground state. It requires relatively little effort to sub-divide the Wilson states. This is an important advantage over NRG which can't change the energy width of the Wilson energy cells $\mathfrak{C}_\nu$. This procedure is discussed in appendix C.

A Wilson's s-electron basis

Wilson [15] in his Kondo paper considered an s-band with a constant density of states and the Fermi energy in the center of the band. By measuring the energy from the Fermi level and dividing all energies by the Fermi energy Wilson obtained a band ranging from -1 to $+1$. To treat the electrons close to the Fermi level at $\zeta = 0$ as accurately as possible he divided the energy interval $(-1:0)$ at energies of $-1/\Lambda, -1/\Lambda^2, -1/\Lambda^3, ..$ i.e. $\zeta_\nu = -1/\Lambda^\nu$. This yields energy cells $\mathfrak{C}_\nu$ with the range $\{-1/\Lambda^{\nu-1} : -1/\Lambda^\nu\}$ and the width $\Delta_\nu = \zeta_\nu - \zeta_{\nu-1}$ $= 1/\Lambda^\nu$. Generally the value $\Lambda = 2$ is chosen. (There are equivalent intervals for positive ζ-values where ν is replaced by $(N-\nu)$ but we discuss here only the negative energies). The new Wilson states c_ν^* are a superposition of all states in the energy interval $(\zeta_{\nu-1}, \zeta_\nu)$ and have an (averaged) energy $(\zeta_\nu + \zeta_{\nu-1})/2 = \left(-\dfrac{3}{2}\right)\dfrac{1}{2^\nu}$, i.e. $-\frac{3}{4}, -\frac{3}{8}, -\frac{3}{16}, .., -\frac{3}{2\cdot 2^{N/2}}, -\frac{1}{2\cdot 2^{N/2}}$. (I count the energy cells and the Wilson states from $\nu = 1$ to N). This spectrum continues symmetrically for positive energies. The essential advantage of the Wilson basis is that it has an arbitrarily fine energy spacing at the Fermi energy.

Wilson rearranged the original quasi-continuous electron states $\varphi_k^\dagger$ in such a way that only one state within each cell $\mathfrak{C}_\nu$ had a finite interaction with the impurity. Assuming that the interaction of the original electron states $\varphi_k^\dagger$ with the impurity is k-independent this interacting state in $\mathfrak{C}_\nu$ had the form

$$c_\nu^\dagger = \textstyle\sum_{\mathfrak{C}_\nu} \varphi_k^\dagger / \sqrt{Z_\nu}$$

where Z_ν is the total number of states $\varphi_k^\dagger$ in the cell $\mathfrak{C}_\nu$ ($Z_\nu = Z(\zeta_\nu - \zeta_{\nu-1})/2$, Z is the total number of states in the band). There are $(Z_\nu - 1)$ additional linear combinations of the states $\varphi_k^\dagger$ in the cell $\mathfrak{C}_\nu$ but they have zero interaction with the impurity and were ignored by Wilson, as they are within this work.

B Construction of the Basis $a_0^\dagger$, $a_i^\dagger$

For the construction of the state $a_0^\dagger$ and the rest of basis $a_i^\dagger$ one starts with the s-band electrons $\left\{c_\nu^\dagger\right\}$ which consist of N states (for example Wilson's states). The $d^\dagger$-state is ignored for the moment.

- In step (1) one forms a normalized state $a_0^\dagger$ out of the s-states with:

$$a_0^\dagger = \sum_{\nu=1}^{N} \alpha_0^\nu c_\nu^\dagger \tag{10}$$

The coefficients α_0^ν can be arbitrary at first. One reasonable choice is $\alpha_0^\nu = 1/\sqrt{N}$

- In step (2) $(N-1)$ new basis states $\overline{a}_i^\dagger$ $(1 \le i \le N-1)$ are formed which are normalized and orthogonal to each other and to $a_0^\dagger$.
- In step (3) the s-band Hamiltonian H_0 is constructed in this new basis. One puts the state $a_0^\dagger$ at the top so that its matrix elements are H_{0i} and H_{i0}.
- In step (4) the $(N-1)$-sub Hamiltonian which does not contain the state $a_0^\dagger$ is diagonalized. This transforms the rest of the basis $\left\{\overline{a}_i^\dagger\right\}$ into a new basis $\left\{a_0^\dagger, a_i^\dagger\right\}$ (but keeps the state $a_0^\dagger$ unchanged). The resulting Hamilton matrix for the s-band then has the form

$$H_0 = \begin{pmatrix} E(0) & V_{fr}(1) & V_{fr}(2) & ... & V_{fr}(N-1) \\ V_{fr}(1) & E(1) & 0 & ... & 0 \\ V_{fr}(2) & 0 & E(2) & ... & 0 \\ .. & ... & ... & ... & ... \\ V_{fr}(N-1) & 0 & 0 & ... & E(N-1) \end{pmatrix} \tag{11}$$

The creation operators of the new basis are given by the set $\left\{a_0^\dagger, a_i^\dagger\right\}$, $(0 < i \le N-1)$. The $a_i^\dagger$ can be expressed in terms of the s-states; $a_i^\dagger = \sum_{\nu=1}^{N} \alpha_i^\nu c_\nu^\dagger$. The state $a_0^\dagger$ uniquely determines the other states $a_i^\dagger$. The state $a_0^\dagger$ is coupled through the matrix elements $V_{fr}\left(i\right)$ to the states $a_i^\dagger$, which makes the state $a_0^\dagger$ an artificial Friedel resonance. The matrix elements $E\left(i\right)$ and $\mathrm{V}_{fr}\left(i\right)$ are given as

$$E(i) = \sum_\nu \alpha_i^\nu \varepsilon_\nu \alpha_i^\nu$$

$$V_{fr}\left(i\right) = \textstyle\sum_\nu \alpha_0^\nu \varepsilon_\nu \alpha_i^\nu$$

- In the final step (5) the state $a_0^\dagger$ is rotated in the N-dimensional Hilbert space. In each cycle the state $a_0^\dagger$ is rotated in the $\left(a_0^\dagger,a_{i_0}^\dagger\right)$ plane by an angle θ_{i_0} for $1 \leq i_0 \leq N-1$. Each rotation by θ_{i_0} yields a new $\overline{a_0}^\dagger$

  $$\overline{a_0}^\dagger = a_0^\dagger \cos\theta_{i_0} + a_{i_0}^\dagger \sin\theta_{i_0}$$

  The rotation leaves the whole basis $\left\{a_0^\dagger, a_i^\dagger\right\}$ orthonormal. Step (4), the diagonalization of the $(N-1)$-sub Hamiltonian, is now much quicker because the $(N-1)$-sub-Hamiltonian is already diagonal with the exception of the i_0- row and the i_0-column . For each rotation plane $\left(a_0^\dagger,a_{i_0}^\dagger\right)$ the optimal $a_0^\dagger$ with the lowest energy expectation value is determined. This cycle is repeated until one reaches the absolute minimum of the energy expectation value. In the example of the Friedel resonance Hamiltonian this energy agrees numerically with an accuracy of 10^{-15} with the exact ground-state energy of the Friedel Hamiltonian [35]. For the Kondo impurity the procedure is stopped when the expectation value changes by less than 10^{-10} during a full cycle.

C Changing the Wilson Basis

In NRG one usually constructs the Wilson states with $\Lambda = 2$. This means that one uses energy cells whose width reduced by a factor of two. NRG is in principle exact for $\Lambda \approx 1$ (together with the requirement that one can diagonalize matrices of gigantic sizes). In the FAIR method we also begin the calculation with $\Lambda = 2$. When the FAIR state $a_0^\dagger$ is obtained for $\Lambda = 2$ in the basis $\left\{c_\nu^\dagger\right\}$ then it is also approximately known in the original basis $\left\{\varphi_k^\dagger\right\}$ (with 10^{23} states)

$$a_0^\dagger = \sum_{\nu=1}^N \alpha_0^\nu c_\nu^\dagger = \sum_{\nu=1}^N \alpha_0^\nu \sum_{\mathfrak{C}_\nu} \varphi_k^\dagger / \sqrt{Z_\nu}$$

Now one can choose a smaller Λ, for example $\Lambda = \sqrt{2}$ and interpolate with good accuracy the FAIR state for the smaller value of Λ [33]. The optimization of the resulting FAIR state requires now a relatively short additional numerical iteration. For the calculation of the Friedel oscillation a value of $\Lambda = \sqrt[4]{2} = 1.19$ was used.

D Geometrical derivation of the Friedel ground state

If the conduction electrons are described by a basis of N states then together with the d-state this yields an $(N+1)$-dimensional Hilbert space $\mathfrak{H}_{N+1}$. The Friedel Hamiltonian is a single particle Hamiltonian and possesses in our case $(N+1)$ orthonormal eigenstates $b_j^\dagger$ which are compositions of the N states $c_\nu^\dagger$ and the one d state $d^\dagger$. The n-electron ground state is then the product of the n creation operator $b_j^\dagger$ with the lowest energy (applied to the vacuum state Φ_0). These n states define the n-dimensional occupied sub-Hilbert space $\mathfrak{H}_n$. The remaining

$(N+1-n)$ eigenstates form the complementary unoccupied sub-Hilbert space $\mathfrak{H}_{N+1-n}$. In the following we treat the creation operators as unit vectors within the Hilbert space.

Now the vector $\mathbf{d}$ of the d state lies partially in the occupied and the unoccupied sub-Hilbert space. It has a projection $\mathbf{d}_1'$ in the occupied sub-Hilbert space $\mathfrak{H}_n$ and a projection $\mathbf{d}_2'$ in the unoccupied sub-Hilbert space $\mathfrak{H}_{N+1-n}$ (so that $\mathbf{d} = \mathbf{d}_1' + \mathbf{d}_2'$). The lengths of the vectors $\mathbf{d}_1'$ and $\mathbf{d}_2'$ are less than one. So we normalize them to $\mathbf{d}_1$ and $\mathbf{d}_2$ with $|\mathbf{d}_i| = 1$. These two vectors are orthogonal (they lie in different sub-Hilbert spaces) and form therefore a two-dimensional space. The vector $\mathbf{d}$ lies within this plane because

$$\mathbf{d} = \mathbf{d}_1' + \mathbf{d}_2' = \alpha\mathbf{d}_1 + \beta\mathbf{d}_2$$

The vector perpendicular to $\mathbf{d}$ in this plane is the FAIR state $\mathbf{a}_0$ with the composition

$$\mathbf{a}_0 = \beta\mathbf{d}_1 - \alpha\mathbf{d}_2$$

Then the vector $\mathbf{d}_1$ has the form

$$\mathbf{d}_1 = \beta\mathbf{a}_0 + \alpha\mathbf{d}$$

The vector $\mathbf{d}_1$ can be used as a basis vector of the $(N+1)$ Hilbert space $\mathfrak{H}_{N+1}$. It lies completely within the occupied sub-Hilbert space. Now we divide the occupied sub-Hilbert space $\mathfrak{H}_n$ into the one-dimensional space $\mathbf{d}_1$ and an $(n-1)$-dimensional subspace $\mathfrak{S}_{n-1}$ which is orthogonal to $\mathbf{d}_1$. This subspace $\mathfrak{S}_{n-1}$ is also orthogonal to the d state vector $\mathbf{d}$ and is therefore built only of $\mathbf{c}_\nu$ vectors. It can be decomposed into $(n-1)$ orthonormal basis vectors $\overline{\mathbf{a}}_i$.

Returning to the physics, the ground state can be expressed as

$$\Psi_F = \left(\beta a_0^\dagger + \alpha^{d}\dagger\right) \prod_{i=1}^{n-1} \overline{a}_i^\dagger \Phi_0$$

Similarly the sub-Hilbert space $\mathfrak{H}_{N+1-n}$ can be divided into $\mathbf{d}_2$ and a sub-space $\mathfrak{S}_{N-n}$ orthogonal to $\mathbf{d}_2$ which is therefore also orthogonal to $\mathbf{d}$. $\mathfrak{S}_{N-n}$ can be expressed in terms of $(N-n)$ orthonormal basis vectors $\overline{\mathbf{a}}_i$ (which consists only of vectors $\mathbf{c}_\nu$).

The creation operators $\overline{a}_i$ are not yet uniquely determined. That is done by diagonalizing the Hamiltonian H_0 in $\mathfrak{S}_{n-1}$ and $\mathfrak{S}_{N-n}$. This yields the new basis $\left\{a_i^\dagger, 1 \leq i < N-1\right\}$. It is straight forward to show that the matrix elements $\left\langle a_i^\dagger \left| H_0 \right| a_{i'}^\dagger \right\rangle$ for $a_i^\dagger \in \mathfrak{S}_{n-1}$ and $a_{i'}^\dagger \in \mathfrak{S}_{N-n}$ vanish as well. (We know the matrix elements of H_F between any state in $\mathfrak{S}_{N-n}$ and any state in $\mathfrak{S}_{n-1}$ vanishes because the two sub-Hilbert spaces are built from a different sub-set of eigenstates of H_F. Therefore $\left\langle a_i^\dagger \left| H_F \right| a_{i'}^\dagger \right\rangle = 0$ if $a_i^\dagger \in \mathfrak{S}_{n-1}$ and $a_{i'}^\dagger \in \mathfrak{S}_{N-n}$. Since $\mathfrak{S}_{n-1}$ and $\mathfrak{S}_{N-n}$ are orthogonal to $d^\dagger$ the d component of the Hamiltonian H_F vanishes anyhow and the remaining part $\left\langle a_i^\dagger \left| H_0 \right| a_{i'}^\dagger \right\rangle = 0$ vanishes for all pairs of i and i'.)

References

[1] J. Friedel, Philos. Mag. 43, 153 (1952); Adv. Phys. 3, 446 (1954); Philos. Mag. Suppl. 7, 446 (1954); Can. J. Phys. 34, 1190 (1956); Nuovo Cimento Suppl. 7, 287 (1958); J. Phys. Radium 19, 573 (1958)

[2] P. W. Anderson, Phys. Rev. 124, 41 (1961)

[3] J. Kondo, Prog. Theor. Phys. 32, 37 (1964)

[4] K. Yosida, Phys. Rev. 147, 223 (1966)

[5] C. M. Varma and Y. Yafet, Phys. Rev. B13, 2950 (1976)

[6] K. Schoenhammer, Phys. Rev. B 13, 4336 (1976)

[7] M. D. Daybell, and W. A. Steyert, Rev. Mod. Phys. 40, 380 (1968)

[8] A. J. Heeger, in Solid State Physics, ed. by F. Seitz, D. Turnbull, and H. Ehrenreich (Academic, New York, 1969), Vol 23, p284

[9] M. B. Maple, in ”Magnetism”, edited by G. T. Rado and H. Suhl (Academic, New York, 1973), Vol. V, p. 289

[10] P. W. Anderson, Rev. Mod. Phys. 50, 191 (1978)

[11] G. Gruener and A. Zavadowski, Prog. Low Temp. Phys. 7B, 591 (1978)

[12] P. Coleman, J. Magn. Magn. Mat. 47, 323 (1985)

[13] A. C. Hewson, The Kondo problem to heavy Fermions, Cambridge University Press, 1993

[14] P. W. Anderson, J. Phys. C3, 2436 (1970)

[15] K. G. Wilson, Rev. Mod. Phys. 47, 773 (1975)

[16] H. O. Frota and L. N. Oliveira, Phys. Rev. B33, 7871 (1986)

[17] H. R. Krishna-murthy, J. W. Wilkins, and K. G. Wilson, Phys. Rev. B 21, 1003 (1980)

[18] H. R. Krishna-murthy, J. W. Wilkins and K. G. Wilson, Phys. Rev. B 21, 1044 (1980)

[19] P. Nozieres, J. Low Temp. Phys. 17, 31 (1974)

[20] P. Nozieres, Ann. Phys. (Paris) 10, 19 (1985)

[21] D. M. Newns and N. Read, Adv. in Phys. 36, 799 (1987)

[22] O. Gunnarsson and K. Schoenhammer, Phys. Rev. B28, 4315 (1983)

[23] N. E. Bickers, Rev. Mod. Phys. 59, 845 (1987)

[24] P. B. Wiegmann, in Quantum Theory of Solids, edited by I. M. Lifshits (MIR Publishers, Moscow, 1982), p. 238

[25] N. Andrei, K. Furuya, and J. H. Lowenstein, Rev. Mod. Phys. 55, 331 (1983)

[26] P. Schlottmann, Phys. Reports 181, 1 (1989)

[27] J. Nilsson, A. H. C. Neto, F. Guinea, and N. M. R. Peres, Phys. Rev. Lett. 97, 266801 (2006)

[28] G. Bergmann, Phys. Rev. B 73, 092418 (2006)

[29] G. Bergmann, Phys. Rev. B 74, 144420 (2006)

[30] G. Bergmann and L. Zhang, Phys. Rev. B 76, 064401 (2007)

[31] G. Bergmann, Phys. Rev. B 77, 104401 (2008)

[32] I. Affleck, L. Borda, H. Saleur, Phys. Rev. B 77, 180404(R) (2008)

[33] G. Bergmann, Phys. Rev. B 78, 195124 (2008)

[34] G. Bergmann, Eur. Phys. J. B2, 233 (1998)

[35] G. Bergmann, Z. Physik B102, 381 (1997)

[36] J. R. Schrieffer and P. A. Wolff, Phys. Rev. 149, 491 (1967)

[37] S. K. Kwon and B. I. Min, Phys. Rev. Lett. 84, 3970 (2000)

[38] R. B. Sahu and L. Kleinman, Phys. Rev. B67, 094424 (2003)

[39] M. E. McHenry, J. M. MacLaren, D. D. VVendensky, M. E. Eberhart and M. L. Prueitt, Phys. Rev. B40, 10111 (1989)

[40] R. Podloucky, R. Zeller and P. H. Dederichs, Phys. Rev. B22, 5777 (1980)

[41] V. I. Anisimov and P. H. Dederichs, Solid State Commun. , 84, 241 (1992)

[42] O. Gunnarsson and K. Schoenhammer, Phys. Rev. B31, 4815 (1985)

[43] J. B. Boyce, and C. P. Slichter, Phys. Rev. Lett. 32, 61 (1974)

[44] I. Affleck, and P. Simon, Phys. Rev. Lett. 86, 2854 (2001)

[45] I. P. Simon and I. Affleck, Phys. Rev. Lett. 89, 206602 (2002)

[46] R. G. Pereira, N. Laflorencie, I. Affleck, and B. I. Halperin, arXiv:cond-mat/0612635 (2007)

[47] J. Simonin, arXiv:0708. 3604 (2007)